Biosensors and Bioelectronics 66 (2015) 356–362

Contents lists available at ScienceDirect

Biosensors and Bioelectronics

journal homepage: www.elsevier.com/locate/bios

Ultrasensitive electrochemical immunosensor for carbohydrate antigen 19-9 using Au/porous graphene nanocomposites as platform and Au@Pd core/shell bimetallic functionalized graphene nanocomposites as signal enhancers

Fan Yang, Zhehan Yang, Ying Zhuo, Yaqin Chai *, Ruo Yuan *

Key Laboratory of Luminescence and Real-Time Analytical Chemistry, Education Ministry, College of Chemistry and Chemical Engineering, Southwest University, Chongqing 400715, PR China

ARTICLE INFO

Article history:
Received 15 July 2014
Received in revised form
18 October 2014
Accepted 29 October 2014
Available online 31 October 2014

Keywords:
Au nanoparticles functionalized porous graphene
Au@Pd core/shell bimetallic functionalized graphene
Immunosensor
Carbohydrate antigen 19-9.

ABSTRACT

A facile and feasible sandwich-type electrochemical immunosensor for ultrasensitive determination of Carbohydrate antigen 19-9 (CA19-9) was designed by using Au nanoparticles functionalized porous graphene (Au-PGO) as sensing platform and Au@Pd core/shell bimetallic functionalized graphene nanocomposites (Au@Pd-Gra) as signal enhancers. Herein, Au@Pd-Gra with a large surface area was prepared for immobilizing plentiful of redox probe-thionine (Thi), horseradish peroxidase (HRP) and secondary antibodies (Ab2), leading to the formation of Au@Pd-Gra/Thi-Ab2/HRP bioconjugate which exhibited satisfying electrochemical redox activity, high electrocatalytic activity and friendly biocompatibility. With the synergistic effect between Au@Pd-Gra and HRP, almost triple amplified detection signal was achieved in the presence of H_2O_2, so as to improve the detection limit of the proposed immunosensor effectively. Furthermore, Au-PGO was utilized as the biosensor platform which could greatly enhance the surface area to immobilize a large amount of captured primary antibodies (Ab1) leading a further enhancement in the sensitivity of immunosensor. Under optimal conditions, the electrochemical immunosensor exhibited desirable performance for determination of CA19-9 with a wide linearity in the range from 0.015 to 150 U mL^{-1} and a relatively low detection limit of 0.006 U mL^{-1}. Importantly, the resulted immunosensor displayed good specificity and high sensitivity, implying potential applications in clinical research.

1. Introduction

Carbohydrate antigen 19-9 (CA19-9) is one of the most important carbohydrate tumor markers in human serum and elevated in many malignancies, such as pancreatic, colorectal, gastric and hepatic carcinomas (Monaghan et al., 2009; Du et al., 2003). The determination of serum CA19-9 levels plays a significant role in early clinical diagnosis, preoperative staging, assessment of resectability and evaluating the recovery of patients (Marrelli et al., 2009; Faraggi and Kramar, 2000). Presently, the clinical measurement of CA19-9 mainly depends on enzyme-linked immunoassay (Gooneilleke and Siriwardena, 2007), radioimmunoassay (Villano et al., 1983) and chemiluminescent immunoassay (Lin and Ju, 2005). However, conventional immunoassay methods always have some disadvantages, such as being time-consuming, poor precision, and difficulty in realizing automation (Ghindilis et al., 1998), resulting in the need for other new, efficient, and easily automated methods for immunoassay.

Electrochemical immunosensors, combining the convenience of electrochemical transduction and the specificity of the immunological reaction, have attracted considerable attention in immunochemical field for its intrinsic advantages such as good portability, low cost and high sensitivity (Chen et al., 2005; Li et al., 2014). In the previous work (Holford et al., 2012; Marquette and Blum, 2006), some of the most significant advances have been reported, including development of electrochemical immunosensors for more sensitivity, stability and accuracy, with lower unit costs, automation, reusability and ease of use. With this approach, electrochemical immunosensors as diagnostic tools have provided a promising technology for the detection of cancer biomarkers. However, it is still a challenge to explore new strategies for improvement of the sensitivity and simplification of the immunosensors.

* Corresponding authors. Fax: +86 23 68253172.
E-mail addresses: yqchai@swu.edu.cn (Y. Chai), yuanruo@swu.edu.cn (R. Yuan).

http://dx.doi.org/10.1016/j.bios.2014.10.066
0956-5663/

Recently, some attempts have been made to enhance the sensitivity of detection by increasing the sensing surface area. Nanomaterials for fabrication of biosensors have contributed a lot in increasing the sensing surface area and amplifying the signal output. For example, a sensitive immunosensor was developed by using G4-polyamidoamine dendrimer-encapsulated Au nanoparticles (NPs) as an effective platform to immobilize larger amounts of target protein (An et al., 2012). Porous graphene oxide (PGO), owning to their tailored pore size distribution, controllable pore structure, and large surface area, have gained wide interest in biosensing for biomolecular immobilization (Wu et al., 2007). Au NPs functionalized PGO (Au-PGO) have been investigated to enhance the surface-to-volume ratio, biocompatibility and stability (Yan et al., 2013). Inspired by the above points, there is great potential for using Au-PGO as a sensing platform.

Besides, many nanomaterials with intrinsic peroxidase-like activity have been widely used in signal amplified immunosensors, owing to their perfect catalytic performance (Bai et al., 2011a, 2011b; Su et al., 2013), such as FeS nanosheets (Dai et al., 2009), SeO_2 NPs (Asati et al., 2009), Fe_3O_4 magnetic NPs (Kim et al., 2011; Liu et al., 2014), and bimetallic NPs (Hou et al., 2014; Lee et al., 2009). As a new class of enzyme mimics, nanomaterials not only possess many extraordinary properties, but also can overcome some of the intrinsic disadvantages of natural enzymes. Bimetallic NPs with alloy or core–shell structures are attractive materials because of their unique optical, electronic, catalytic, and magnetic properties (Toshima and Yonezawa, 1998). Further efforts are being directed toward the synthesis of various bimetallic NPs for applications in biosensors, photonic devices, and catalysis (Lee et al., 2008). For example, Au–Pd bimetallic NPs have been reported to construct a novel electrochemical immunosensor for the detection of alpha fetoprotein (AFP), in which Au–Pd bimetallic NPs with catalytic activity and highly conductive graphene sheets were used for signal amplification (Zhao et al., 2013). Pt–Au bimetallic NPs have been reported to develop an ultrasensitive electrochemical aptasensor for signal amplification (Bai et al., 2011a, 2011b). Recently, it was demonstrated that $Au_{core}Pd_{shell}$ (Au@Pd) bimetallic NPs were successfully dispersed on graphene by a simple one step reducing method (Chen et al., 2011). More importantly, the Au@Pd functionalized graphene (Au@Pd-Gra) have superior peroxidase-like catalytic activity. However, to the best of our knowledge, there is no report focusing on Au@Pd-Gra as label application for electrochemical sandwich-type immunosensor.

In this work, we designed a novel sandwich-type electrochemical immunosensor for the detection of CA19-9 based on Au-PGO as effective sensing platform and Au@Pd-Gra as signal enhancers. On one hand, Au@Pd-Gra was employed for immobilizing some amounts of mediator Thi, Ab2 and HRP, forming the signal probes of Au@Pd-Gra/Thi-Ab2/HRP bioconjugates. On the other hand, Au-PGO was first prepared and introduced as the immobilization matrix for binding of biomolecules. Through "sandwich" reaction, the target protein CA19-9 was sandwiched between the primary antibody and the prepared Au@Pd-Gra/Thi-Ab2/HRP bioconjugates, resulting in a detectable signal. According to the electrocatalytic current signal, quantificational detection of CA19-9 could be achieved successfully. Details of the preparation, characterization and possible application of immunosensor are discussed as follows.

2. Experimental

2.1. Reagents and material

CA19-9 antibody (anti-CA19-9) and CA19-9 (0–250 U mL^{-1}) were purchased from Biocell Company (Zhengzhou, China). Graphene Oxide (GO) was purchased from Nanjing Xianfeng nano Co. (Nanjing, China). $HAuCl_4 \cdot 4H_2O$, Palladium acetate ($Pd(OAC)_2$), thionine (Thi), bovine serum albumin (BSA, 96–99%), N-(3-dimethylaminopropyl)-N′-ethylcarbodiimidehydrochloride (EDC) and N-hydroxysuccinimide (NHS) were obtained from Sigma Chem. Co. (St. Louis, MO, USA). Polyethyleneglycol (PEG), trisodium citrate, and ascorbic acid (AA) were obtained from Kelong Chemical Inc. (Chengdu, China). Horseradish peroxidase (HRP) was purchased from Sinopharm Chemical Reagent Co. (Shanghai, China). Hydrogen peroxide (H_2O_2, 30% *w/v* solution) was obtained from Chemical Reagent Co. (Chongqing, China). Phosphate buffer solutions (PBS) (0.1 M, pH 7.4) were prepared using 0.1 M Na_2HPO_4, 0.1 M KH_2PO_4 and 0.1 M KCl. Ferricyanide solutions ($Fe(CN)_6^{3-/4-}$, 5.0 mM) were obtained by dissolving potassium ferricyanide and potassium ferrocyanide with PBS (pH 7.4). The prepared solutions were kept at 4 °C before use. The working buffer was composed of a 0.1 M HAc–NaAc buffer containing 0.1 M KCl. All other chemicals were of reagent grade and were used as received. Double distilled water was used throughout this study.

2.2. Apparatus

Cyclic voltammetry (CV), electrochemical impedance spectroscopy (EIS) and differential pulse voltammetry (DPV) measurements were carried out with a CHI 660 C electrochemistry workstation (Shanghai CH Instruments, China). All experiments which were performed with a conventional cell contained a platinum wire as auxiliary electrode, a saturated Ag/AgCl electrode as reference electrode and the modified glassy carbon electrode (GCE, Φ=4 mm) as working electrode. X-ray photoelectron spectroscopy (XPS) measurements were carried out on a VG Scientific ESCALAB 250 spectrometer, using Al Ka X-ray (1.486.6 eV) as the light source. The size and morphology of nanoparticles were estimated from a transmission electron microscopy (TEM) (JEM-2100, JEOL, Japan) and a scanning electron microscope (SEM) (S-4800, Hitachi, Japan). The value of pH was measured by pH meter (MP 230, Mettler-Toledo, Switzerland).

2.3. Synthesis of Au-PGO

The Au-PGO was prepared using the following procedure according to the literature with a slight modification (Yan et al., 2013). At first, graphene oxide (GO) was dissolved in double distilled water by ultrasonication for 1 h with a concentration of 5 mg mL^{-1}. Then, the homogeneous GO dispersion (10 mL, 0.5 mg mL^{-1}), 200 μL $HAuCl_4 \cdot 4H_2O$ (1%, *w/w*) and 20 μL PEG (1%, *w/w*) were mixed uniformly and sonicated for 1 h. Subsequently, the mixture was reacted at 180 °C for 12 h. After cooling down to room temperature, the mixture was washed three times with double distilled water. Finally, the Au-PGO was obtained through freeze drying process. The formation of a columnar ice phase and subsequent drying produced the porous graphene structures of a few microns in diameter. The resulting Au-PGO was redispersed in PBS.

2.4. Synthesis of Au@Pd-Gra

Au@Pd-Gra was prepared by the following steps according to the literature (Chen et al., 2011) with a slight modification: trisodium citrate (0.28 g) was firstly added to 45 mL GO suspension

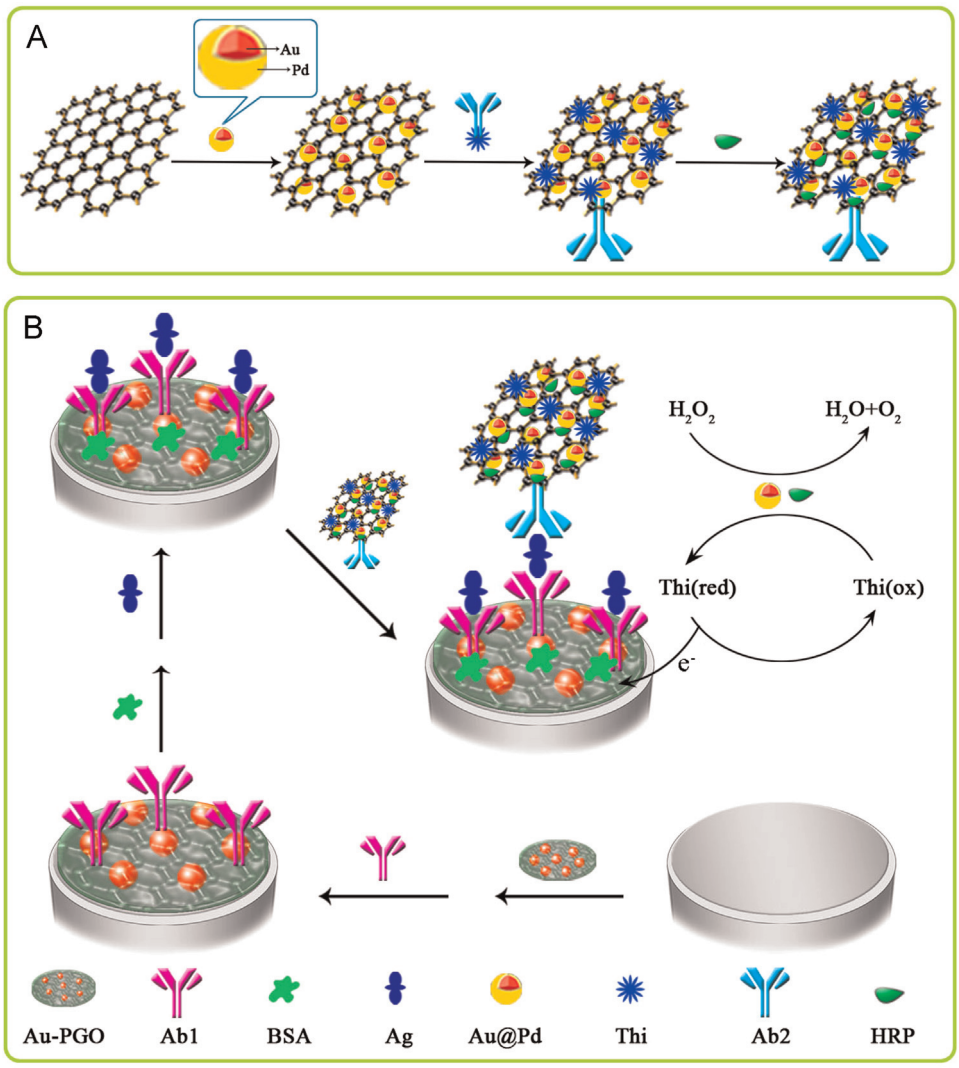

Scheme 1

Scheme 1. (A) Preparation procedure of Ab2 bioconjugate (Au@Pd-Gra/Thi-Ab2/HRP). (B) Schematic illustration of stepwise immunosensor fabrication process and the signal amplification mechanism.

(0.6 mg mL^{-1}) and sonicated for 30 min. Then, the mixture was heated to 100 °C in an oil bath. Meanwhile, 8.6 mg $Pd(OAC)_2$, 0.6 mL (20 mM) $HAuCl_4 \cdot 4H_2O$ and 2.3 mL (0.1 M) AA were added to the mixture subsequently. The mixture was heated at 100 °C with stirring for 2.5 h. After cooling to room temperature, the mixture (Au@Pd-Gra) was washed extensively with double distilled water and centrifuged several times. Finally, the products of Au@Pd-Gra were dispersed in 5 mL of double distilled water.

2.5. Preparation of Au@Pd-Gra/Thi-Ab2/HRP bioconjugate

Immobilization of Ab2, Thi and HRP onto Au@Pd-Gra was completed according to the following steps (Scheme 1A): firstly, 40 mg EDC and 10 mg NHS were used as coupling agents to conjugate the antibodies with redox probes by the formation of an amide link between the carboxyl of anti-CA19-9 and the amino of thionine (Thi-Ab2). The antibody–redox probe conjugates were gently stirred for 12 h and centrifuged for 15 min at 8000 rpm at 4 °C. Then, 200 μL of Thi-Ab2 was added into 1 mL homogeneous Au@Pd-Gra suspension under stirring at 4 °C for 8 h. Subsequently, 1 mg HRP was dissolved in Au@Pd-Gra/Thi-Ab2 solution and incubated at 4 °C for 4 h, followed by centrifugation. Finally, Au@Pd-Gra/Thi-Ab2/HRP bioconjugate was dispersed in 1 mL PBS and stored at 4 °C for further use.

2.6. Fabrication of proposed immunosensor

Prior to the preparation procedure, the GCE (Φ=4 mm) was firstly polished with 0.3 and 0.05 μm alumina slurry to obtain a mirror-like surface, followed by successive sonication with double distilled water and ethanol, and then dried at room temperature. After the cleansing procedure, 10 μL of prepared Au-PGO solution was first poured on the GCE surface and dried slowly in air. Next, Au-PGO/GCE was immersed into a solution of anti-CA19-9 (Ab1) for 12 h at 4 °C. Following that, Ab1/Au-PGO/GCE was washed with double distilled water to remove the physically absorbed species and then incubated in 15 μL of 0.25% BSA for 30 min at 37 °C to block the possible remaining active sites and to avoid non-specific adsorption, followed by washing with double distilled water. The proposed immunosensor was stored at 4 °C when not in use. Based on the sandwich format, the resulting immunosensor was incubated with 15 U mL^{-1} CA19-9 samples for 40 min at 25 °C, and then immersed in the prepared Au@Pd-Gra/Thi-Ab2/HRP bioconjugate solution for immunoreaction, followed by washing

with PBS to remove the unbound Ab2 bioconjugates. The stepwise assembly of the proposed immunosensor is shown in Scheme 1B.

2.7. Experimental measurements

The electrochemical properties of the working electrode were characterized by CV, EIS and DPV measurements. CV and EIS measurements of the electrode fabrication were performed in 2 mL of 5 mM $Fe(CN)_6^{3-/4-}$ solution with the potential range from −0.2 to 0.6 V at a scan rate of 50 mV s^{-1}. CV and DPV measurements were performed in 2 mL of 0.1 M working buffer (pH 5.5) containing 1.5 mM H_2O_2 to investigate the performance of the immunosensor. The DPV parameters applied were 50 mV pulse amplitude, 50 ms pulse width, 0.2 s pulse period and a voltage range from −0.4 to 0 V.

3. Results and discussion

3.1. Electrochemical characterization of the immunosensor

The cyclic voltammetry (CV) is an effective method for probing the process of electrode modification. CVs of the stepwise modified processes of the proposed electrode were performed in $Fe(CN)_6^{3-/4-}$ solution. As shown in Fig. 1A, curve a exhibited a well-defined redox wave, corresponding to the reversible redox reaction of ferricyanide ions on the bare GCE. The Au-PGO/GCE (curve b) had larger current than bare GCE (curve a), which ascribed to the fact that Au-PGO could significantly enhance the effective surface area and facilitate the electron transfer (Wu et al., 2014). Peak current decreased clearly after Ab1 was assembled on the AuNPs layer (curve c), indicating that the capture antibody as an electron-transfer blocking layer can severely hinder the diffusion of ferricyanide toward the electrode surface (Fan et al., 2015). Subsequently, when non-electroactive BSA was used to block nonspecific sites, the peak current further decreased (curve d) (Jie et al., 2007). The peak current decreased with the CA19-9 immobilization on the electrode (curve e), which was consistent with the fact that the hydrophobic layer of the protein insulated the conductive support.

Electrochemical impedance spectroscopy (EIS) was employed to further investigate the stepwise modified processes of the proposed electrode. Fig. 1B shows the Nyquist plots of impedance spectra at different electrodes in $Fe(CN)_6^{3-/4-}$ solution. The semicircle diameter in the impedance spectrum equals to the electron-transfer resistance (R_{et}). As seen from curve a, only a small semicircle could be observed at the bare GCE, indicating a low transfer resistance. Subsequently, Au-PGO was deposited on the surface of GCE, the diameter of semicircle was decreased, implying that the film of Au-PGO enhanced the electron transfer in the electrochemical probe (curve b). When Ab1 captured antibodies were assembled onto the Au-PGO/GCE, the resistance was increased (curve c). After BSA blocking and subsequent immobilization of CA19-9, the resistance increased gradually as the experiment proceeded (curve d and e), which was consistent with the fact that the hydrophobic layer of the protein insulated the conductive support and perturbed the interfacial electron transfer.

3.2. Comparison of different signal amplification strategies

Signal amplification is critical to obtain high sensitivity and low detection limit for the sandwich-type electrochemical immunosensor (Wang, 2006). To investigate the signal amplification of the proposed protocol, the immunosensors were utilized for the detection of CA19-9 with three types of labeled probes, including Thi-Ab2/HRP bioconjugate, Au@Pd-Gra/Thi-Ab2 bioconjugate and Au@Pd-Gra/Thi-Ab2/HRP bioconjugate (Fig. 2). During the measurement process, the same batch immunosensors were incubated with 15 U mL^{-1} CA19-9 in the absence and presence of H_2O_2. The black line (curve a) and red line (curve b) in Fig. 2 shows CVs before and after the addition of 1.5 mM H_2O_2, respectively. As shown in Fig. 2, the use of Au@Pd-Gra/Thi-Ab2 bioconjugate (Fig. 2B) offered greater current shift than that obtained with Thi-Ab2/HRP bioconjugate (Fig. 2A). The experiment result confirmed that Au@Pd-Gra exhibits efficient catalysis towards H_2O_2 than that of directly using HRP-labeled secondary antibody, illustrating the good peroxidase-like catalytic activity. More inspiringly, it can be found that the use of Au@Pd-Gra/Thi-Ab2/HRP bioconjugate offers highest current shift (Fig. 2C) than those obtained with other two labeled probes, suggesting the excellent catalytical amplification of the proposed bioconjugate. The high signal amplification of the Au@Pd-Gra/Thi-Ab2/HRP bioconjugate may be attributed to the synergistic action of Au@Pd-Gra and HRP could extremely amplify the electrochemical signal. Accordingly, Au@Pd-Gra/Thi-Ab2/HRP bioconjugate was chosen as a tracer for sandwich-type immunosensor to obtain superior signal amplification for the following experiments.

3.3. Quantificational detection of CA19-9

Under the optimal conditions, the analytical performance of the prepared immunosensor was studied toward different CA19-9

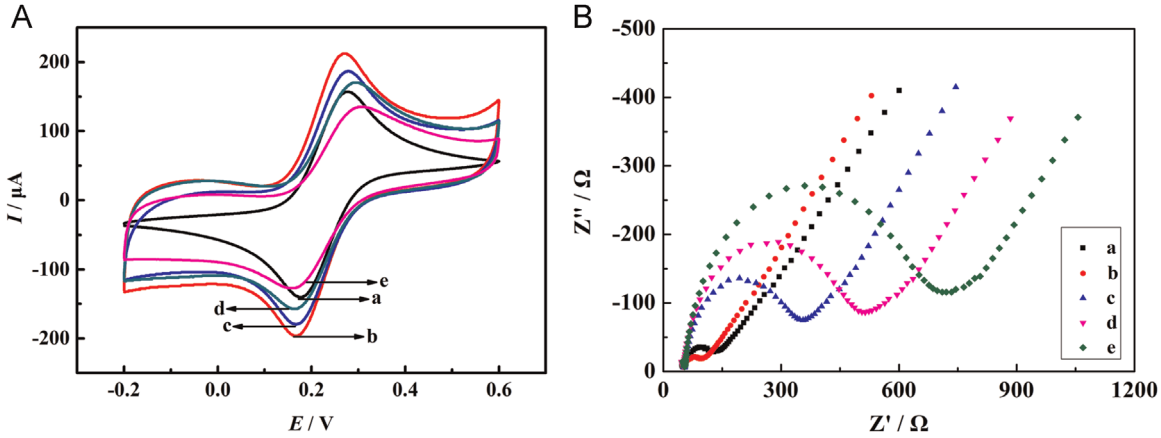

Fig. 1. The CVs (A) and EIS (B) of different electrodes performed in pH 7.4 PBS containing 5 mM $Fe(CN)_6^{3-/4-}$ and 0.1 M KCl: (a) bare GCE; (b) Au-PGO/GCE; (c) Ab1/Au-PGO/GCE; (d) Ab1/Au-PGO/GCE blocked with 0.25% BSA and (e) the proposed immunosensor incubated with CA19-9. The scan rate was 50 mV s^{-1} and all potentials are given versus SCE.

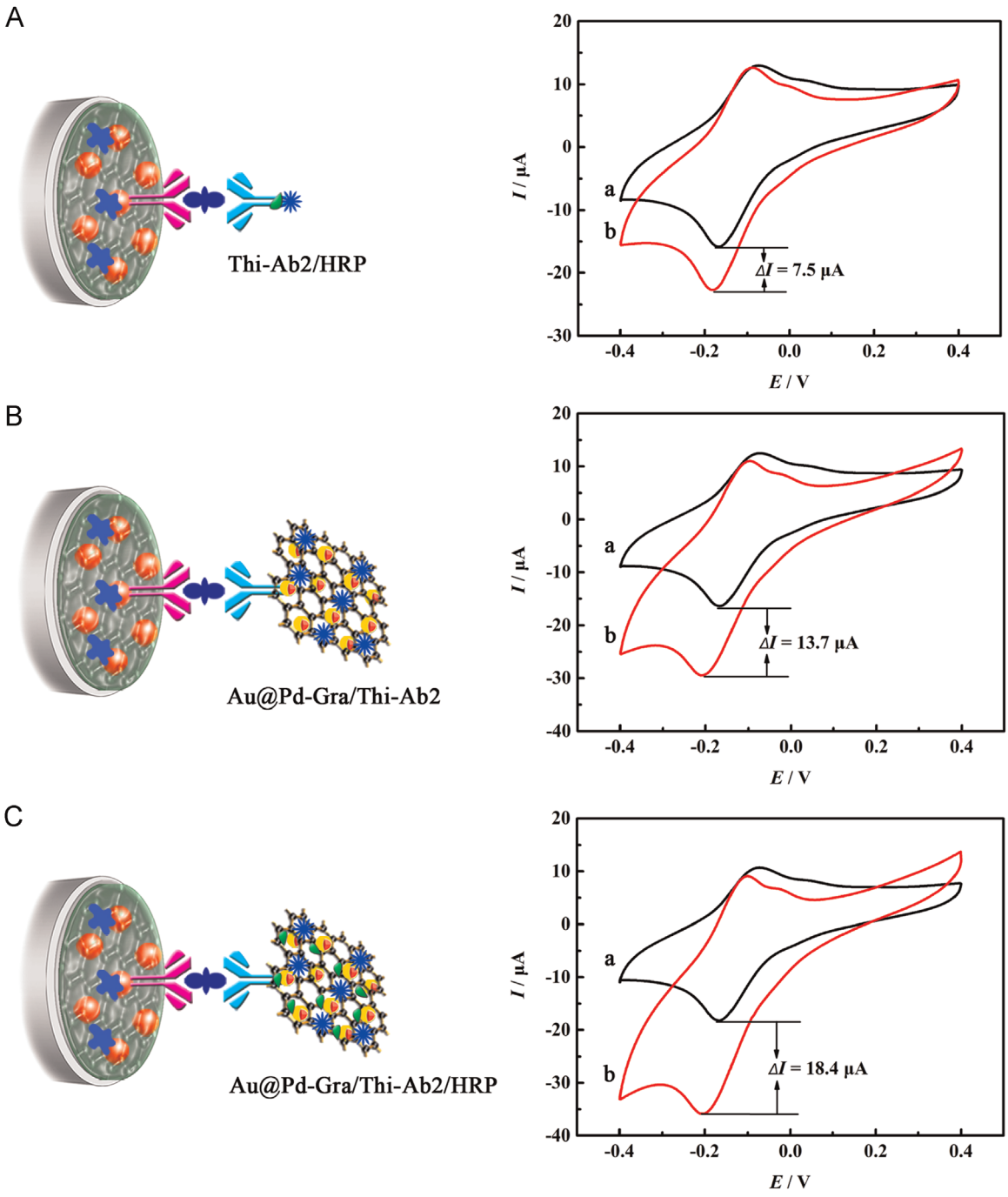

Fig. 2. CVs of the different sandwich format immunosensors in the absence (curve a, black line) and in the presence of 1.5 mM H_2O_2 (curve b, red line) in 0.1 M working buffer (pH 5.5) by using various signal tags: Thi-Ab2/HRP bioconjugate, Au@Pd-Gra/Thi-Ab2 bioconjugate and Au@Pd-Gra/Thi-Ab2/HRP bioconjugate. (For interpretation of the references to color in this figure legend, the reader is referred to the web version of this article.)

standards in pH 5.5 working buffer containing 1.5 mM H_2O_2 by using Au@Pd-Gra/Thi-Ab2/HRP bioconjugate as trace and H_2O_2 as enzyme substrate with a sandwich-type immunoassay format. As indicated from Fig. 3A, the DPV peak currents of the electrochemical immunoassay increased with the increase of CA19-9 concentrations, and exhibited a linear relationship between the DPV peak currents and the CA19-9 concentration in the range from 0.015 to 150 U mL^{-1} (Fig. 3B). The regression equation was I (μA)=26.1924+9.8328 × log $c_{CA19\text{-}9}$ (U mL^{-1}, R^2=0.9982) with a detection limit of 0.006 U mL^{-1} (S/N=3). These results indicated that the prepared immunosensor detection for CA19-9 was reliable and sensitive for the determination of CA19-9 concentrations.

3.4. Specificity, reproducibility, and stability of the immunosensor

Specificity is a very important characteristic and it is necessary to check it for the developed immunoassay method. To monitor the binding selectivity of the proposed immunosensor to CA19-9 (0.15 U mL^{-1} was chosen as sample), we challenged the system with several other tumor markers: carcinoma antigen-125 (CA125, 15 U mL^{-1}), carbohydrate antigen 15-3 (CA15-3, 15 U mL^{-1}), and prostate-specific antigen (PSA, 15 U mL^{-1}). Significantly higher current response was observed with the target CA19-9 than with other biomarkers (Fig. 4). Moreover, the presence of high concentration of interfering components (CA125, CA15-3 and PSA)

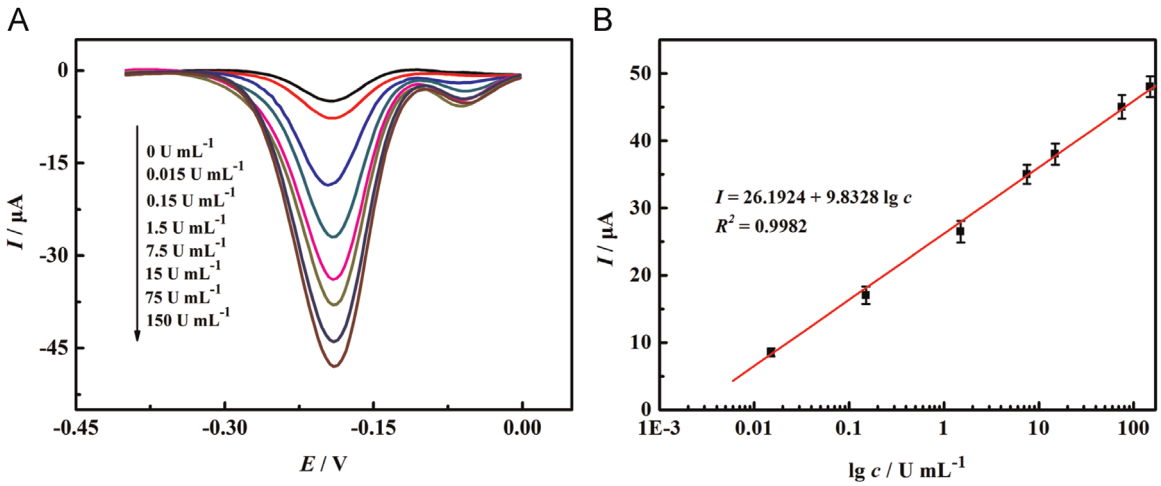

Fig. 3. (A) DPV responses of the proposed immunosensor after incubation with different concentrations of CA19-9 under optimal conditions. (B) Calibration curve for determination of CA19-9 using Au@Pd-Gra/Thi-Ab2/HRP bioconjugate for signal amplification (error bars: SD, $n=3$).

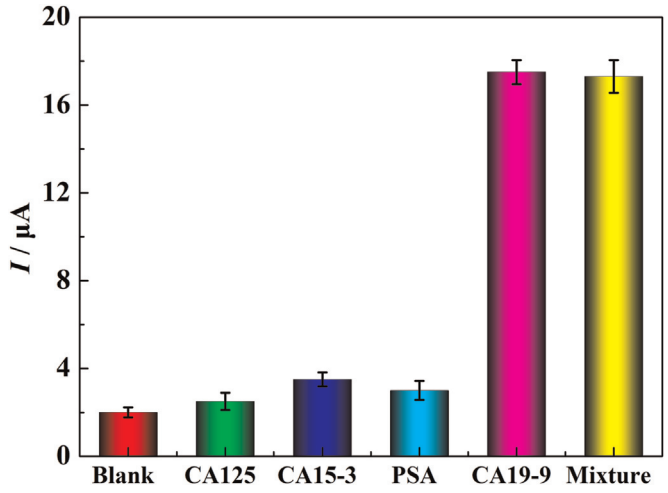

Fig. 4. Specificity of the immunosensor toward: (a) zero analyte; (b) 15 U mL^{-1} CA125; (c) 15 U mL^{-1} CA15-3; (d) 15 U mL^{-1} PSA; and (e) the admixture was consisted of CA19-9, CA125, CA15-3 and PSA.

also did not interfere with the assay for CA19-9 (0.15 U mL^{-1}). These results clearly indicated the high specificity of the proposed assay for CA19-9 detection.

Simultaneously, the reproducibility of the proposed immunosensor was investigated by the intra- and inter-assays. All the relative standard deviations (RSD) for the intra- and inter-assay were not more than 5%. The experimental results suggested the acceptable reproducibility of the proposed immunosensor.

Furthermore, the stability of the immunosensor was also examined. When the prepared electrodes were not in use, they were stored in PBS (pH 7.4) at 4 °C. It can be seen that 94.8% of the initial response remained after one week and 87.3% of the initial response remained after 30 days, which indicated that the developed immunosensor had acceptable stability.

3.5. *Preliminary application for real sample and method validation*

In order to evaluate the feasibility application of the proposed immunosensor in clinical analysis, the method was challenged by detecting 8 human serum samples (obtained from Xinqiao Hospital, Chongqing, China) from cancer patients. The CA19-9 contents of these samples were assayed using the developed immunosensor and the referenced chemiluminescent immunoassay, respectively. Statistical comparison of the experimental results is summarized in Table 1. (Note: The analytes with higher original concentrations in the samples were appropriately diluted.) The relative deviations between the proposed method and the chemiluminescent immunoassay for CA19-9 in 8 human serum samples were found to vary from −6.64% to 6.20%. Compared with the previously reported immunosensor (Lin et al., 2004) for CA19-9 detection, the detection results of this method were more accurate. Assays on serum from normal individuals clearly indicated that this proposed method was suitable for the analysis of real samples in clinical diagnosis.

4. Conclusions

In summary, this manuscript described a novel and ultrasensitive electrochemical immunoassay for the detection of CA19-9 by using Au-PGO as a sensing platform and the combination of Au@Pd-Gra and HRP for signal amplification. Highlights of this

Table 1
Experimental results comparison of two methods obtained in serum samples.

Sample no.	Found by chemiluminescent immunoassay [a]/U mL^{-1}	Found by the immunosensor [a]/U mL^{-1}	Relative standard deviation/%
1	8.00	8.20	2.50
2	16.80	16.50	−1.80
3	31.00	32.90	6.20
4	47.20	49.40	4.66
5	54.20	50.60	−6.64
6	64.20	66.90	4.20
7	83.30	81.20	−2.52
8	113.30	116.80	3.10

[a] The values shown here are the average values from three measurements.

work can be summarized as follows: (i) Au-PGO on electrode not only facilitated electrons transfer but also provided a large accessible surface area for the immobilization of abundant Ab1. (ii) Au@Pd-Gra with high aspect ratio could increase the amount of redox probes, thus enhancing the response signals. Moreover, with the synergistic amplifying action produced from Au@Pd-Gra and HRP, the proposed immunosensor exhibited extraordinary electrochemical biocatalysis in the presence of thionine toward H_2O_2, which largely increased the sensitivity of proposed immunosensor. In addition, experimental results indicated that the electrochemical immunoassay exhibited high sensitivity, acceptable reproducibility and stability. In view of these advantages, the novel and powerful immunosensor has a great potential application in the area of disease diagnostics and clinical analysis.

Acknowledgments

The authors are grateful for the National Natural Science Foundation of China (21075100, 21275119), the Ministry of Education of the People's Republic of China (Project 708073), Specialized Research Fund for the Doctoral Program of Higher Education (20110182120010), the Natural Science Foundation Project of Chongqing (CSTC-2011BA7003, CSTC-2010BB4121), the Fundamental Research Funds for the Central Universities (XDJK2013A008, XDJK2014A012), China and Department of Clinical Laboratory, Xinqiao Hospital, Third Military Medical University (Chongqing, China).

Appendix A. Supplementary Information

Supplementary data associated with this article can be found in the online version at.

References

An, Y.R., Jiang, X.L., Bi, W.J., Chen, H., Jin, L.T., Zhang, S.P., Wang, C.G., Zhang, W., 2012. Biosens. Bioelectron. 32, 224–230.
Asati, A., Santra, S., Kaittanis, C., Nath, S., Perez, M.J., 2009. Angew. Chem. Int. Ed. 48, 2308–2312.
Bai, L.J., Yuan, R., Chai, Y.Q., Yuan, Y.L., Zhuo., Y., Mao, L., 2011a. Biosens. Bioelectron. 26, 4331–4336.
Bai, L.J., Yuan, R., Chai, Y.Q., Yuan, Y.L., Mao, L., Wang, Y., 2011b. Anal. Chim. Acta 698, 14–19.
Chen, J., Yan, F., Dai, Z., Ju, H.X., 2005. Biosens. Bioelectron. 21, 330–336.
Chen, H.Y., Li, Y., Zhang, F.B., Zhang, G.L., Fan, X.B., 2011. J. Mater. Chem. 21, 17658–17661.
Dai, Z.H., Liu, S.H., Bao, J.C., Ju, H.X., 2009. Chem. – Eur. J. 15, 4321–4326.
Du, D., Yan, F., Liu, S.L., Ju, H.X., 2003. J. Immunol. Methods 283, 67–75.
Fan, H.X., Guo, Z.K., Gao, L., Zhang, Y., Fan, D.W., Ji, G.L., Du, B., Wei, Q., 2015. Biosens. Bioelectron. 64, 51–56.
Faraggi, D., Kramar, A., 2000. Urol. Oncol. 5, 211–213.
Ghindilis, A.L., Atanasov, P., Wilkins, M., Wilkins, E., 1998. Biosens. Bioelectron. 13, 113–131.
Gooneilleke, K.S., Siriwardena, A.K., 2007. Eur. J. Surg. Oncol. 33, 266–270.
Holford, T.R.J., Davis, F., Higson, S.P.J., 2012. Biosens. Bioelectron. 34, 12–24.
Hou, L., Gao, Z.Q., Xu, M.D., Cao, X., Wu, X.P., Chen, G.N., Tang, D.P., 2014. Biosens. Bioelectron. 54, 365–371.
Jie, G.F., Liu, B., Pan, H.C., Zhu, J.J., Chen, H.Y., 2007. Anal. Chem. 79, 5574–5581.
Kim, M.I., Shim, J., Li, T.H., Lee, J., Park, H.G., 2011. Chem. – Eur. J. 17, 10700–10707.
Lee, Y.W., Kim, M., Kim, Z.H., Han, S.W., 2009. J. Am. Chem. Soc. 131, 17036–17037.
Lee, Y.W., Kim, N.H., Lee, K.Y., Kwon, K., Kim, M., Han, S.W., 2008. J. Phys. Chem. C 112, 6717–6722.
Li, W.P., Li, L., Ge, S.G., Song, X.R., Ge, L., Yan, M., Yu, J.H., 2014. Biosens. Bioelectron. 56, 167–173.
Lin, J.H., Ju, H.X., 2005. Biosens. Bioelectron. 20, 1461–1470.
Lin, J.H., Yan, F., Hu, X.Y., Ju, H.X., 2004. J. Immunol. Methods 291, 165–174.
Liu, Y., Yuan, M., Qiao, L.J., Guo, R., 2014. Biosens. Bioelectron. 52, 391–396.
Marrelli, D., Caruso, S., Pedrazziani, C., Neri, A., Fernandes, E., 2009. Am. J. Surg. 198, 333–339.
Marquette, C.A., Blum, L.J., 2006. Biosens. Bioelectron. 21, 1424–1433.
Monaghan, P.J., Leonard, M.B., Neithercut, W.D., Raraty, M.G.T., Sodi, R., 2009. Clin. Chim. Acta 406, 41–44.
Su, H.C., Zhao, H., Qiao, F.M., Chen, L.J., Duan, R.H., Ai, S.Y., 2013. Analyst 138, 3026–3031.
Toshima, N., Yonezawa, T., 1998. New J. Chem. 22, 1179–1201.
Villano, B.C.D., Brennan, S., Brock, P., Bucher, C., Liu, V., 1983. Clin. Chem. 29, 549–552.
Wang, J., 2006. Biosens. Bioelectron. 21, 1887–1892.
Wu, S., Ju, H.X., Liu, Y., 2007. Adv. Funct. Mater. 17, 585–592.
Wu, X.Y., Chai, Y.Q., Yuan, R., Zhuo, Y., Chen, Y., 2014. Sens. Actuators B: Chem. 203, 296–302.
Yan, M., Sun, G.Q., Liu, F., Lu, J.J., Yu, J.H., Song, X.R., 2013. Anal. Chim. Acta 798, 33–39.
Zhao, L.F., Li, S.J., He, J., Tian, G.H., Wei, Q., Li, H., 2013. Biosens. Bioelectron. 49, 222–225.